J Membrane Biol (2015) 248:93–102
DOI 10.1007/s00232-014-9746-9

Salinity-Induced Noise in Membrane Potential of Characeae *Chara australis*: Effect of Exogenous Melatonin

Mary J. Beilby · Sabah Al Khazaaly · Mary A. Bisson

Received: 10 July 2014 / Accepted: 23 October 2014 / Published online: 7 November 2014

Abstract Salt sensitive Characeae *Chara australis* responds to 50 mM NaCl by a prompt appearance of noise in the trans-membrane potential difference (PD). The noise diminishes with time in saline and PD depolarization, leading to altered current–voltage characteristics that could be modeled with H^+/OH^- channels. Beilby and Al Khazaaly (JMB 230:21–34, 2009) suggested that the noise might arise from cooperative transient opening of H^+/OH^- channels. Presoaking cells in 10 μM melatonin over 24 h abolished the noise in some cells, postponed its appearance in others or changed its characteristics. As melatonin is a very effective antioxidant, we postulated opening of H^+/OH^- channels by reactive oxygen species (ROS). Measurement of ROS using dihydrodichlorofluorescein diacetate confirmed substantial reduction in ROS production in melatonin-treated cells in saline and sorbitol media. However, ROS concentration decreased as a function of time in saline medium. Possible schemes for activation of H^+/OH^- channels under salinity stress are considered.

Keywords *Chara* · Saline-induced noise · Salinity stress · H^+/OH^- channels · Reactive oxygen species

M. J. Beilby (✉) · S. Al Khazaaly
School of Physics, University of NSW, Kensington 2052, Sydney, NSW, Australia
e-mail: m.j.beilby@unsw.edu.au

M. A. Bisson
Department of Biological Sciences, University at Buffalo, Buffalo, NY 14260, USA
e-mail: bisson@buffalo.edu

Introduction

Melatonin is a powerful antioxidant of ancient origin, probably introduced into plant and animal kingdoms by cyanobacteria (that became chloroplasts) and purple non-sulfur bacteria (that became mitochondria—Tan et al. 2013). Since 1950s melatonin became generally known for its role in circadian rhythms in animals including humans (Brzezinski 1997). Dubbels et al. (1995) and Hattori et al. (1995) focused attention on plant endogenous melatonin by surveying its content in common fruits and vegetables. Murch et al. (1997) measured melatonin in growing plants and Murch et al. (2000) described a putative pathway for melatonin synthesis in plants. Melatonin and the related metabolite serotonin are derived from tryptophan and indole-3-acetic acid (IAA). The structural similarities of melatonin and serotonin molecules to that of IAA suggest a role for these substances in growth and development (Murch et al. 2001; Murch and Saxena 2002; Murch et al. 2009, 2010; Pelagio-Flores et al. 2012; Tan et al. 2012). The possible involvement of melatonin in plant circadian rhythms is also under investigation (Poggeler et al. 2001; Van Tassel et al. 2001; Wolf et al. 2001; Tan et al. 2007a; Boccalandro et al. 2011).

Our experimental organisms, the Characeae, are closely related to ancestors of all land plants (McCourt et al. 2004; Wodniok et al. 2011; Timme et al. 2012) and have already been used to establish the fundamentals of plant cell electrophysiology (Hope and Walker 1975; Beilby and Casanova 2013) and cytoplasmic streaming (Shimmen 2007). The large cells of the Characeae allow experiments at single cell level, with minimal disturbance to the cell structure. Salt sensitive Characeae *Chara australis* produces endogenous melatonin in similar amounts to leaf and shoot portions of higher plants, such as medicinal herb St. John's wort (Murch et al. 2000).

Lazar et al. (2013) added 10 μM melatonin to the medium and soaked cells overnight, increasing the quantum yield of photochemistry of photosystem II by 34 %. The increased efficiency appears to be due to the greater fraction of open reaction centers of photosystem II, rather than increased efficiency of each reaction center. More open reaction centers reflect better functionality of all photosynthetic transport chain constituents. The authors suggested that melatonin protection against reactive oxygen species (ROS) covers not only chlorophyll, but also photosynthetic proteins in general.

Apart from photosynthesis, many abiotic stresses generate ROS in the cell organelles and cytoplasm (Miller et al. 2010). For instance, Amirjani (2010) measured increasing levels of H_2O_2 in rice seedlings exposed to NaCl between 25 and 200 mM after 13 days.

Chara australis does not survive in comparatively low salinity of 50–100 mM NaCl. The cells die after a few days if the calcium concentration of the saline medium is low (0.1 mM) and within hours if they are exposed to mechanical or electrical stimuli (Shepherd et al. 2008). Beilby and Al Khazaaly (2009) documented the electrophysiological response to salinity and resolved early PD (potential difference) depolarization due to proton pump inhibition, followed by further depolarization, which can be modeled by global activation of H^+/OH^- channels. In the native low salt pond water, the H^+/OH^- channels are part of the pH banding mechanism that enhances the cell's carbon assimilation (see Beilby and Bisson 2012 for review). Under saline stress, global activation of H^+/OH^- channels would dissipate the proton electrochemical gradient that powers the $2H^+/Cl^-$ symport and H^+/Na^+ antiport, necessary for the normal turgor recovery and maintenance of cytoplasmic low Na^+. The H^+/OH^- channels respond promptly upon exposure to salinity: the membrane PD exhibits characteristic noise, thought to originate from transient opening of groups of these channels (Al Khazaaly et al. 2009). The noise diminishes with time in saline and PD depolarization and disappears as the membrane current–voltage (I/V) characteristics change and can be modeled by H^+ (or OH^-) transport (Beilby and Al Khazaaly 2009). The hypothesis that H^+/OH^- channels participate in the saline response is supported by zinc ion inhibition of both the noise and the H^+/OH^- dominated I/V profile (Al Khazaaly and Beilby 2012).

Why are the H^+/OH^- channels activated by saline stress? Bisson and Walker (1980) discovered global activation of H^+/OH^- channels upon increasing the medium pH above 9.0. In this case, the cells survived for many hours and recovered the proton pump dominated state once returned to native medium with low salt and slightly alkaline pH (Bisson and Walker 1980). The salinity-induced H^+/OH^- channel activation proceeds in media of neutral pH, several pH units below the pH activation threshold (Bisson and Walker 1981). In recent experiments Eremin et al. (2013) employed fluorescent probe dihydrodichlorofluorescein (DCHF) to trace ROS formation under strong spot illumination of *Chara* surface. The authors suggest that excess ROS formed in the chloroplasts was carried away by the cytoplasm, oxidizing either histidine or SH (sulfhydryl) groups on transport proteins, leading to opening the H^+/OH^- channels.

In the present work, we exploit the antioxidant potential of melatonin to gain further insight into the electrophysiology of *Chara australis* response to fatal salinity stress.

Table 1 Experimental media

Contents	APW/mM	Melatonin APW/mM	Sorbitol APW/mM	Saline APW/mM
NaCl	1.0	1.0	1.0	50.0
KCl	0.1	0.1	0.1	0.1
$CaCl_2$	0.1	0.1	0.1	0.1
HEPES	5.0	5.0	5.0	5.0
Tris-Base	3.0	3.0	3.0	3.0
Sorbitol			90	
Melatonin		10×10^{-3}		
Measured pH	7.1	7.1	7.1	7.1

Materials and Methods

Cultures

Sydney cell cultures and electrophysiology protocols were described previously in detail (Shepherd et al. 2008; Beilby and Al Khazaaly 2009; Al Khazaaly and Beilby 2012). Briefly, *Chara australis* was collected from golf course lake in Little Bay, Sydney, and grown in round tanks in the laboratory in autoclaved soil covered by Milli-Q water. Tanks were illuminated by Gro-Lux fluorescent tubes providing photosynthetically active radiation of $\sim$80 μmol m^{-2} s^{-1} on day/night cycle of 12/12 h. Young internodal cells (1–2.5 cm in length) were cut off the plants and stored in APW (artificial pond water, see Table 1) several days prior to the experiment. The ROS experiments were performed in Buffalo, NY, on a distinct culture of *C. australis,* grown in soil with Broyer & Barr medium, 40 μmol m^{-2} s^{-1}, on day/night cycle of 12/12 h, as described in Bisson (1984).

Electrical Measurements

The electrical measurements were performed at University of NSW, Sydney. The cell was placed in three-compartment chamber, each compartment insulated by silicone grease. The membrane PD across both plasma membrane

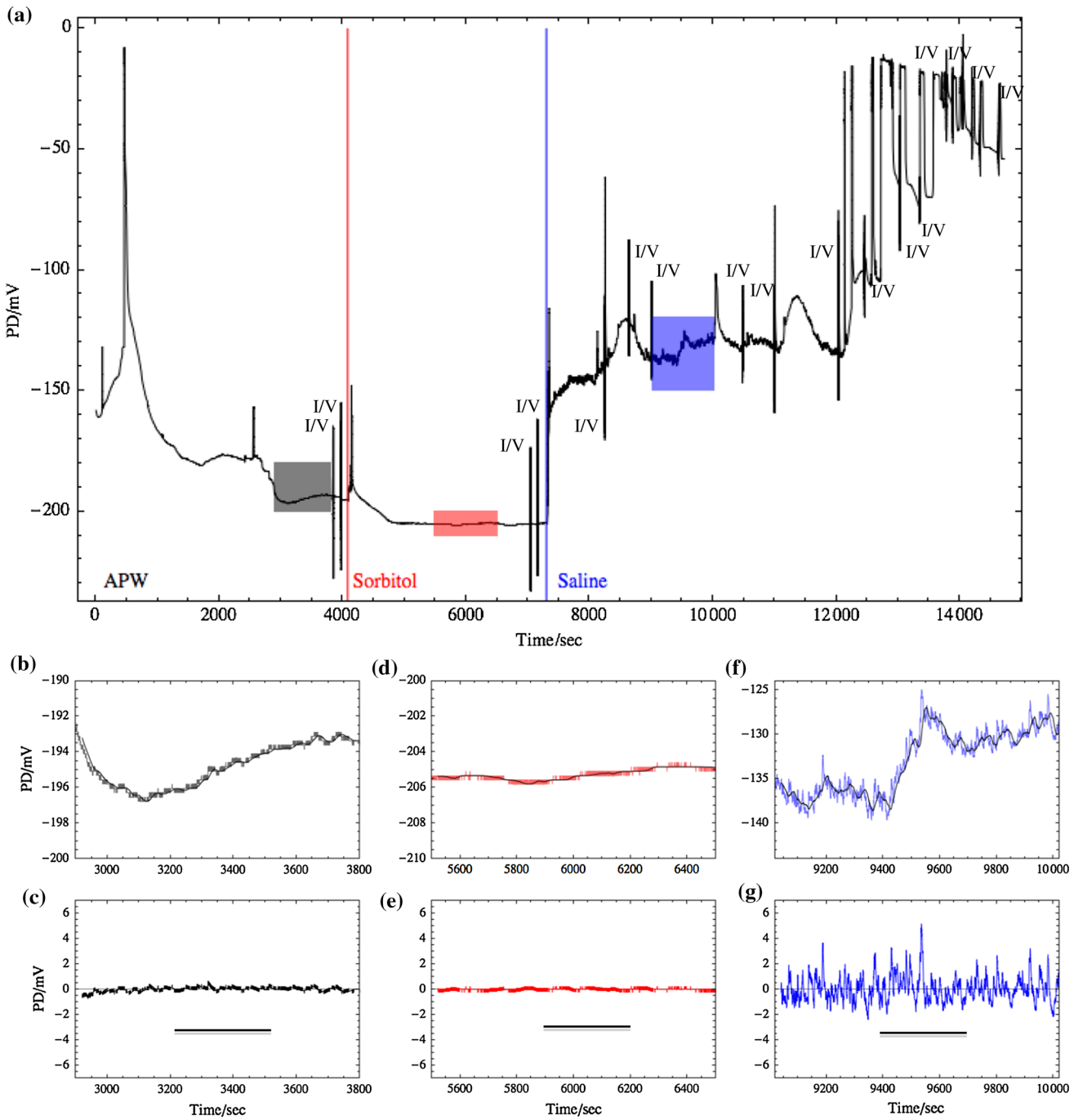

Fig. 1 (**a**) The resting PD of a control cell (13/8/13). The cell recovered from handling and electrode impalement after little more than 60 min (3600 s). The exposure to sorbitol APW (*red line* and "Sorbitol") generated more negative PD. Saline APW (*blue line* and "Saline") resulted in prompt depolarization, but no action potentials (AP). The PD then varied around the −130 mV level for about 1 h, before becoming unstable and moving above −100 mV. The vertical lines designate the I/V scans, which only take 8 s (marked as I/V). APs, spontaneous or after an I/V scan, can also appear as vertical lines. The gray, red, and blue rectangles indicate the windows of ~1,000 points, where the running average ($n = 200$) was calculated and is shown as smooth *black line* in (**b**), (**d**) and (**f**). The "blocky" appearance of the data in APW (*black*) and sorbitol APW (*red*) is due to resolution limit of the A/D, about 0.25 mV. The moving average was subtracted from the data to isolate the "noisiness" of the PD: (**c**), (**e**) and (**g**). The salinity-induced noise is quite marked. The *horizontal bars* designate 5 min time interval (Color figure online)

and tonoplast was voltage clamped by passing current between Ag/AgCl electrodes in the outside compartments and the narrow (5 mm) middle compartment. The I/V characteristics were obtained using bipolar staircase with pulses of 60–100 ms width, separated by 120–250 ms at the resting PD. An LSI11/73 computer data logged at the

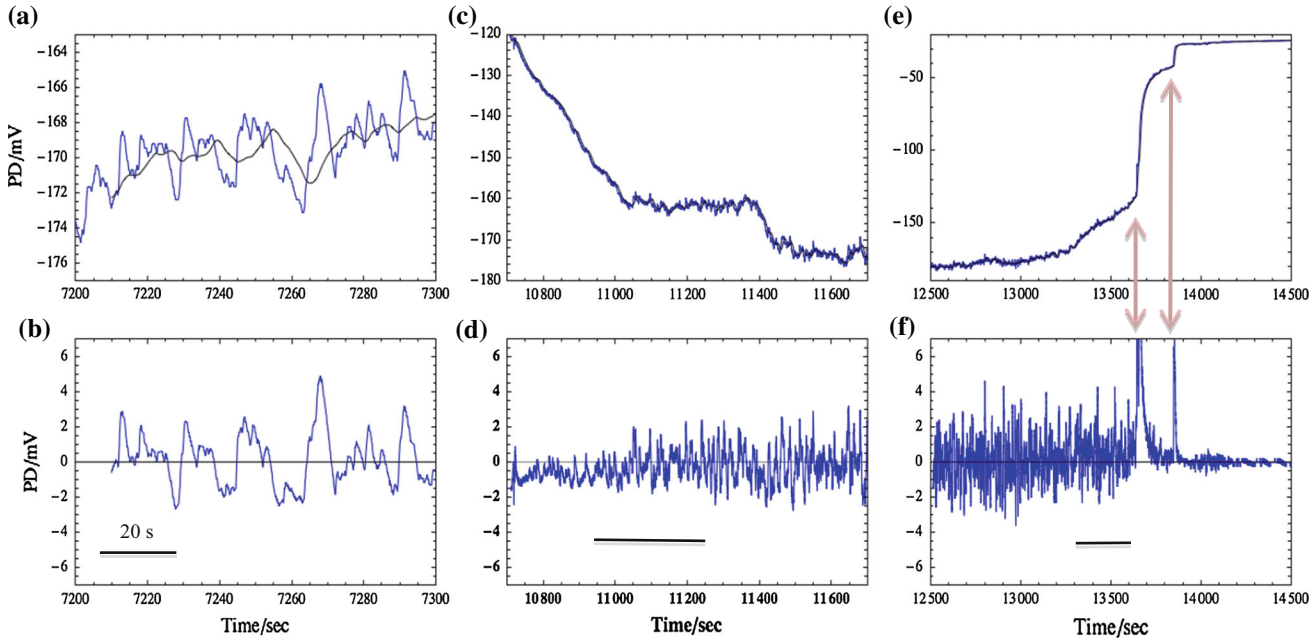

Fig. 2 (**a**) The salinity-induced noise and the running average ($n = 100$) on an expanded time scale.(**b**) The subtracted noise retains its "shape", with n between 50 and 200. (**c**) The salinity-induced noise diminishes after an AP. (**d**) The subtracted noise shows the gradual increase in noise amplitude. The *bar* designates 5 min. (**e**) As the PD depolarizes strongly after almost 2 h exposure to saline, the noise amplitude decreases quite rapidly (**f**). The two *upward* spikes in (**f**) are artifacts due to sudden changes in resting PD (see *red arrows*). The *bar* designates 5 min. The data were collected from control cell (14/6/13) with $n = 100$ for the running average in (**a**), (**c**) and (**e**) (Color figure online)

rate of one measurement/ms. Each I/V scan took 8 s. The resting PD was monitored throughout the experiment by another computer at a rate of 10 points/s.

Experimental Procedure

The cell was placed in the chamber, APW was introduced into all compartments. The vacuolar electrode was inserted and the membrane PD was allowed to stabilize (see Fig. 1a). Usually cells were in this "recovery mode" for several hours. Some cells rejected the electrode and had to be re-impaled. When the PD became steady, the medium in all the compartments was changed to sorbitol APW for at least 1 h. This technique separated the osmotic shock from the Na^+ shock (Shepherd et al. 2008). Saline was then introduced in the compartments and the cell was monitored for several hours (see Fig. 1a).

Analysis

The PD versus time files were downloaded into Mathematica 9 for processing. Running average was computed for selected time windows (~1,000 points) in each medium. The time windows were chosen to avoid sudden changes in the resting PD level, such as an AP, electrode blockage, or an I/V scan (see Fig. 1a). The running (or moving) average was calculated for a fixed subset n (between 50 and 200 points) of the data and the calculation moved progressively through the whole data set (see Fig. 1b, d, f). The average was then subtracted from the data to isolate the higher frequency noise from the longer time trends (see Fig. 1c, e, g). In some cases, the sudden changes in PD could not be avoided, which introduced artefactual spikes into the noise record (see Fig. 2e, f). These artifacts can be identified by comparison to the fitted membrane PD.

Melatonin Treatment

Melatonin stock solution was made from crystalline powder just before use and was added to APW before cell pre-treatment. Cells or explants for H_2O_2 essay were soaked in Melatonin APW in the dark for 24 h. In earlier experiments, the single cells were pretreated in melatonin APW for up to 3 days.

ROS Assay with Fluorogenic Probe Dihydrodichlorofluorescein Diacetate (DCHF-DA)

The experiments were performed at University at Buffalo, NY, and used explants: the top part of Characeae plant with two to three internodes. Explants were cut several days before the experiment, as the process of cutting also increased ROS levels for periods less than 24 h (Bisson, unpublished data). At the start of the experiment, the explants were weighed and between 0.5 and 0.7 g were placed in tubes containing both sorbitol APW and 14.2 nM DCHF-DA in dim light. The control explants were incubated

for 2 h in sorbitol APW/DCHF-DA. The cells exposed to saline APW were incubated for 1 h in sorbitol APW/DCHF-DA (as in electrophysiological experiments) and 1 h in saline APW/DCHF-DA. As change of solution could introduce some amount of oxygenation, the control cells had the same medium poured out after 1 h and poured back into incubation tube. Same procedures were used for explants soaked in Melatonin APW for 24 h. To explore the ROS concentration as a function of time in saline APW, the control explants were again incubated for 2 h in sorbitol APW/DCHF-DA. The cells exposed to saline APW were incubated for 105 min in sorbitol APW/DCHF-DA and 15 min in saline APW/DCHF-DA and 90 min in sorbitol APW/DCHF-DA and 30 min in saline APW/DCHF-DA.

The extraction was performed in cold room at 4 °C. To remove any DCHF cleaved by the esterases in the cell wall, the cells were rinsed in 8 mM $CaCl_2$ and 5 mM MES buffer for ~2 min. The efficacy of this treatment was checked by confocal microscopy for cells incubated in low ionic strength media and in the saline. The fluorescence in the cell wall (and its decrease) was easily identified by the position with respect to the chloroplasts. After rinsing, the explants were blotted and placed in a mortar with small amount of liquid nitrogen. The frozen explants were ground with a pestle. The material was suspended in 40 mM Tris–HCl buffer at pH 7, placed in centrifuge tube and shaken for 5 min. The material was centrifuged for 10 min at 20,000*g*. The supernatant was transferred into a plastic vial and kept cold (but not frozen).

The fluorimeter (Molecular Devices) was calibrated using 0, 25, 50, 75, and 100 nM DCF (oxidized and fluorescing DCHF). Three replicates of 100–200 µl of the standards and the samples were placed in a microwell plate. The excitation wavelength was set to 490 nm and the emission wavelength was set to 520 nm. The errors in sample weight and fluorescence were computed from differences between the three samples. The explants were weighed 3 times in one of the experiments and the absolute error was quite consistent. The errors incurred in transferring the ground explants into centrifuge tubes were difficult to quantify, so two samples were measured for each medium and the data are presented as average. The error arising from the difference between the two samples was greater than the weight and fluorescence combined errors and we chose it as the final error. The two samples were processed consecutively, so the error might be a slight overestimate, especially if the rate of ROS production changed with time.

Results

Characteristics of the Salinity-Induced Noise

Four control cells were exposed to sequence of APW/sorbitol/saline APW (see Table 1 for full media composition). A record of cell (13/8/13) is shown in Fig. 1a. The PD response of this cell to the three media was typical. Further, the PD record was clear and continuous, as the internal electrode has not been rejected by the cell throughout the experiment. Data windows of about 1,000 s are depicted as gray rectangle (APW), red rectangle (sorbitol), and blue rectangle (saline). The membrane PD in each window and the fitted running average (continuous black line) are shown in Fig. 1b, d and f. The subtracted noise levels for each window are displayed in Fig. 1c, e and g. Salinity-induced noise was easy to distinguish in Fig. 1a, f and g. The "structure" of salinity-induced noise was not greatly altered by the subtraction of the running average with n between 50 and 200 (see Fig. 2a, b). The running average in saline APW did show lower frequency oscillation (see, for instance Fig. 1f or Fig. 2a), which was attributed to the same process as the noise (see "Discussion" section). Excitation of an AP diminished salinity-induced noise amplitude in some cells (see Fig. 2c, d). Note the gradual recovery of noise amplitude in Fig. 2d. As the membrane PD depolarized above −100 mV with time in saline, the amplitude of the salinity-induced noise declined (see Fig. 2e, f). Upon change from sorbitol to saline APW, the salinity-induced noise appeared promptly (see Fig. 3a, b), especially if no AP was elicited at the time of the medium change.

The Effects of Melatonin

Total of 14 cells was pretreated in 10 µM melatonin for 24–72 h in the dark. Interestingly, only freshly made melatonin medium applied for 24 h affected the salinity-induced noise: out of 6 cells thus treated, 5 showed (i) no salinity-induced noise, (ii) delay before salinity-induced noise appeared after exposure to saline APW, or (iii) unusual features in salinity-induced noise. The remaining cell exhibited noisy PD in both sorbitol and saline APW and was not included (see "Discussion" section). Figure 3c and d shows the transition from sorbitol to saline APW in melatonin-treated cell (4/2/14). This cell did not exhibit salinity-induced noise at all, but the membrane PD depolarized rapidly and became unstable with repetitive spontaneous APs. Melatonin-treated cell (13/2/14) showed similar time-course of no salinity-induced noise upon medium transition and fast decline to depolarized PD levels above −100 mV. Another melatonin-treated cell (19/6/13) depolarized more slowly and the salinity-induced noise was postponed by 1500 s (25 min) and then gradually increased in amplitude despite the depolarized PD level (Fig. 4). A gradual salinity-induced noise activation was also observed in cell (2/7/13). Cell (14/2/14) exhibited saline-induced noise upon medium change (Fig. 5a, b), but after an AP, the salinity-induced noise was replaced by

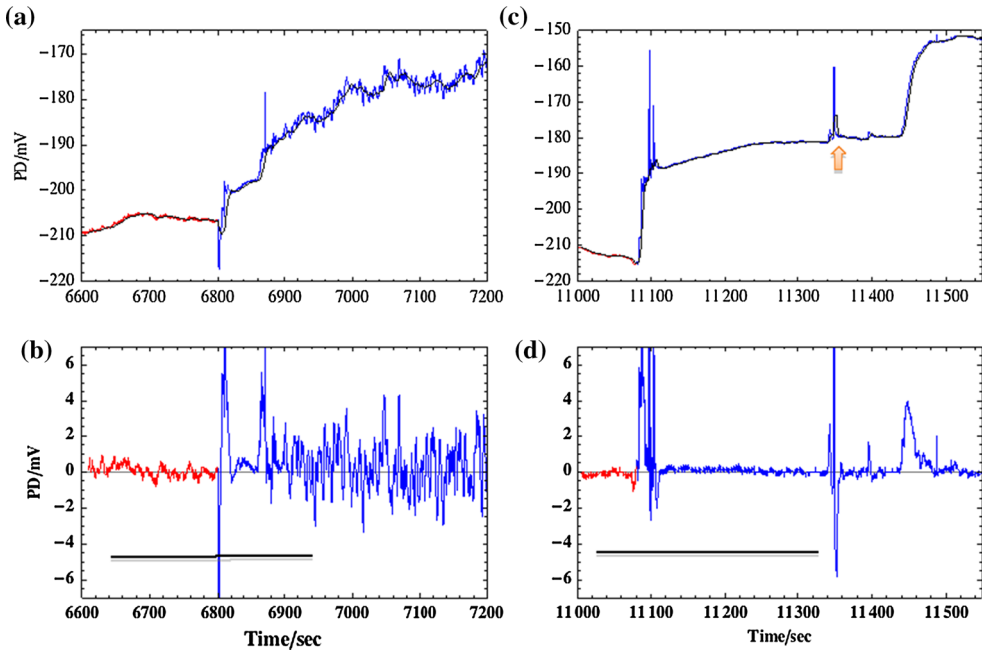

Fig. 3 (**a**) Transition from sorbitol APW (*red*) to saline (*blue*) in control cell (14/6/13). There was no AP, but the resting PD measurement was disrupted by medium change and exhibited spikes between 6800 and 6900 s. The running average was fitted with $n = 100$ (*black line*). (**b**) The subtracted noise: saline-induced noise (*blue*) started promptly after the medium change. The *bar* designates 5 min. There are again artifact spikes, originating from the averaging process, where the resting PD changed abruptly. (**c**) Transition from sorbitol APW (*red*) to saline (*blue*) in melatonin-treated cell (4/2/14). There was no AP, but the medium was refreshed at 11 340 s, causing a spike in resting PD (*red arrow*). The running average was fitted with $n = 50$ (*black line*). (**d**) The amplitude of subtracted PD noise remained constant, except for two artifact spikes due to medium refresh and sudden depolarization of membrane PD at 11440 s. The *bar* designates 5 min (Color figure online)

more isolated spikes (Fig. 5c, d), which became sharper with depolarization (Fig. 5e, f). Similar sharp spikes were also observed in cell (19/7/13) during repolarization after APs in saline APW.

ROS Concentration in the Cells in Sorbitol and Saline APW

Figure 6a shows that ROS production was substantially reduced in melatonin soaked cells in both sorbitol and saline APW. However, ROS production in saline APW did not appear significantly different than that in sorbitol APW. Figure 6b shows that ROS production in saline APW dropped sharply over 30 min.

Discussion

Salinity-Induced Noise

We have made an extensive study of the salinity-induced noise (Al Khazaaly et al. 2009; Al Khazaaly 2011; Al Khazaaly and Beilby 2012). Al Khazaaly (2011) measured salinity-induced noise in about hundred cells that have been exposed to 50 or 100 mM NaCl medium after pre-conditioning in sorbitol APW with matching osmolarity. Only four cells did not exhibit the typical salinity-induced noise, while a larger group of young cells in spring of 2007 had noisy PDs in all media and were excluded from the analysis. Cells with "normal" salinity-induced noise exhibited prompt noise activation upon medium change, transient decrease in noise amplitude after some APs and gradual decrease in noise amplitude upon depolarization above −100 mV with time in saline APW. This decrease coincided with "upwardly concave" I/V characteristics, where the membrane PD response to medium pH could be modeled by H^+/OH^- channels (Beilby and Al Khazaaly 2009). Both the salinity-induced noise and the upwardly concave I/V characteristics were inhibited by $ZnCl_2$ (potent inhibitor of animal H^+ channels) and re-activated by 2-mercaptoethanol (Al Khazaaly and Beilby 2012).

Fourier analysis of PD fluctuations in APW, sorbitol and saline APW in the 1–500 mHz frequency range resulted in $1/f^2$ rise in power as frequency fell, with marked increase in noise power in saline APW, but no distinct peaks of deterministic oscillatory processes (Al Khazaaly et al. 2009). Light smoothing of the data suggested that what appeared as low frequency oscillation

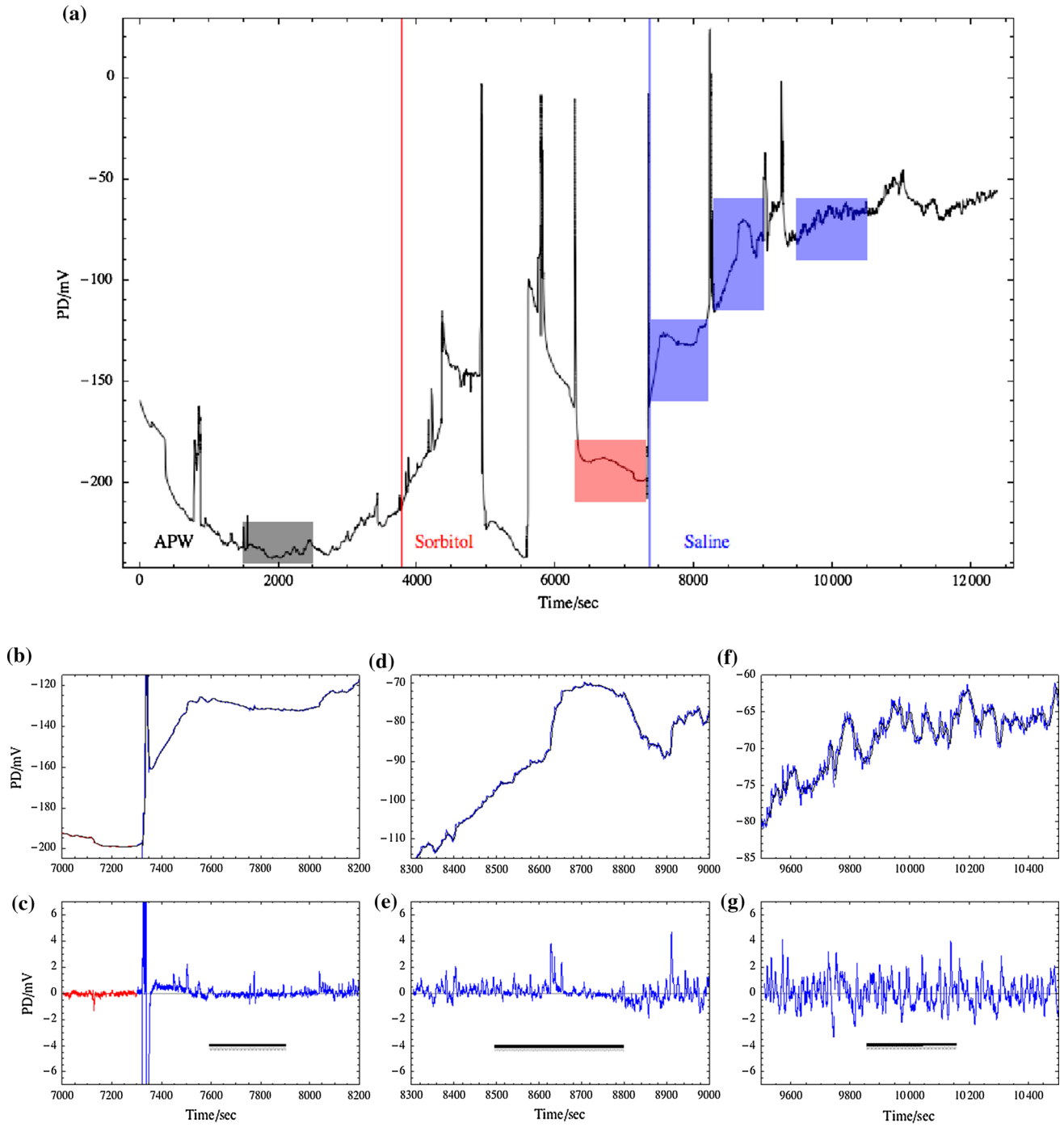

Fig. 4 (**a**) The resting PD in different media for melatonin-treated cell (19/6/13). In this cell, the saline-induced noise was postponed. The *colored rectangles* indicate the data windows, where the noise levels were measured (APW and sorbitol data are not shown). The PD was somewhat noisy in APW and the cell rejected the electrode several times. The PD became quieter in sorbitol. The noise level in sorbitol is shown in *red* in (**b**) and (**c**) for comparison. (**b**) The cell fired an AP upon change to saline and did not exhibit saline-induced noise in 800 s. The running average was fitted with $n = 50$ and subtracted from the data (**c**). The *bar* designates 5 min. (**d**) Despite firing another AP and depolarizing above −100 mV, where saline-induced noise tends to diminish in control cells, the noise level increased (**e**). The running average was fitted with $n = 50$. The *bar* designates 5 min. (**f, g**) The noise level increased even at very depolarized membrane PD. The running average was fitted with $n = 100$. The *bar* designates 5 min (Color figure online)

(see the running averages in Figs. 1f, 2a, 3a), results from the variance of the random processes generating the noise. In the present study, we computed running averages of running averages of the raw data, using larger n and confirmed the random nature of these oscillations (calculations not shown).

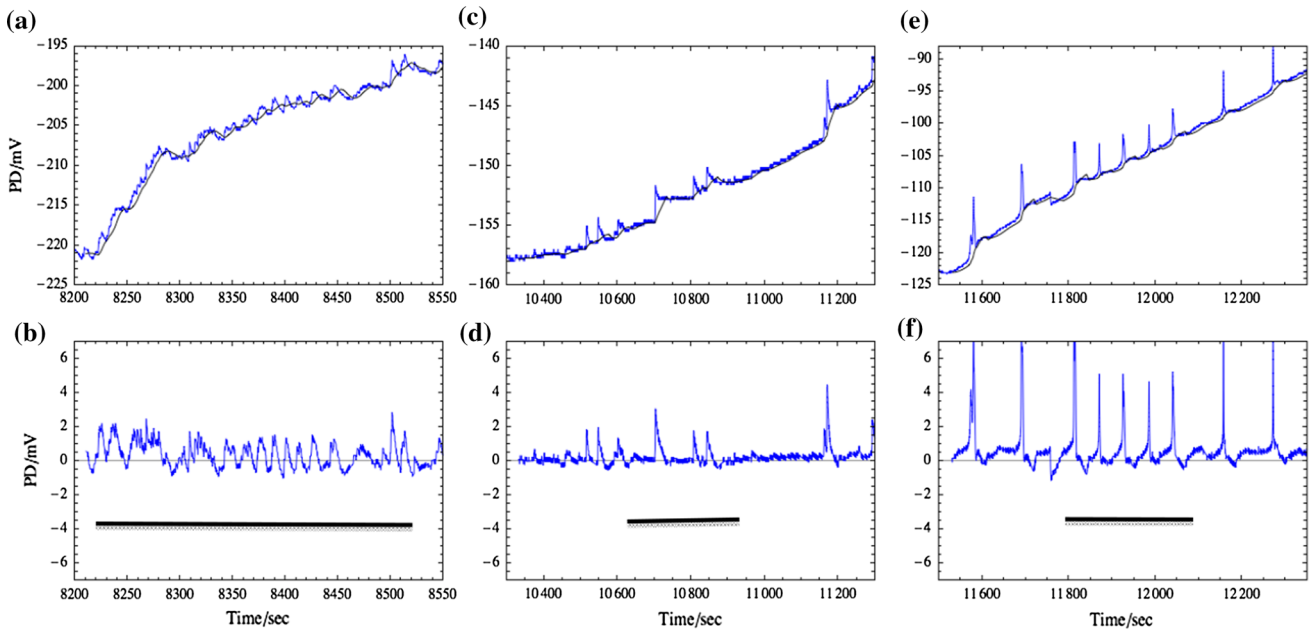

Fig. 5 Unusual evolution of saline-induced noise in melatonin-treated cell (14/2/14). (**a**) Upon exposure to saline medium, the membrane PD exhibited low amplitude saline-induced noise. The PD was fitted with running average ($n = 100$) and noise isolated in (**b**). The *bar* designates 5 min. (**c**) The cell was subjected to I/V profile run and fired an AP afterwards. The saline-induced noise disappeared and recovered partially as a series of widely spaced isolated spikes (**d**). The *bar* designates 5 min. (**e**) As the cell continued to depolarize, the spikes became sharper and their amplitude increased (**f**). The *bar* designates 5 min

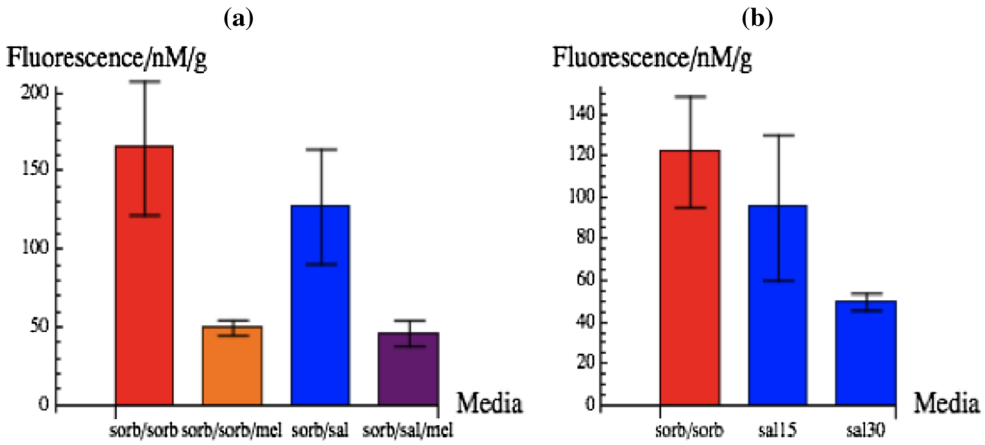

Fig. 6 (**a**) ROS concentration as measured by fluorescence of oxidized DCHF. The control explants were incubated with DCHF for 2 h in sorbitol APW and fluorescence was measured (*red bar*). The orange bar shows the effect of pre-treatment in 10 μM melatonin for 24 h on explants incubated in the same medium. Explants incubated in 1 h sorbitol APW/1 h saline APW (+DCHF-DA) were not significantly different from the sorbitol treatment (*blue bar*). Same treatment but with explants exposed to melatonin APW again shows much lower fluorescence (*purple bar*). (**b**) ROS concentration in saline APW as a function of time. Control cells were again incubated in sorbitol APW/DCHF-DA for 2 h. The cells exposed to saline APW were incubated for 105 min in sorbitol APW/DCHF-DA and 15 min in saline APW/DCHF-DA (sal15) and 90 min sorbitol APW/DCHF-DA and 30 min in saline APW/DCHF-DA (sal30) (Color figure online)

The four control cells in this study exhibited the same prompt salinity-induced noise activation, transient noise amplitude decrease after some APs and gradual amplitude decrease with depolarization (Figs. 2c–f, 3a, b). Cells treated for 24 h in melatonin APW showed no increase in noise level upon transition from sorbitol to saline (Fig. 3c, d), very gradual increase in salinity-induced noise (Fig. 4) or unusual "isolated spikes" in the membrane PD of cell exposed to saline (Fig. 5). Eremin et al. (2013) experiment with oxidized fluorescent DFC established that ROS is generated in the chloroplasts illuminated by strong light and exported into streaming cytoplasm. The authors suggest that ROS activates H^+/OH^- channels, producing an alkaline band downstream from the illuminated area. In the

animal kingdom, the voltage-gated H^+ channels in the brain microglia are activated by H_2O_2 (Wu L 2014). Initially, we hypothesized that the salinity stress leads to increase of ROS production in the cytoplasm, also activating H^+/OH^- channels, initially manifesting as salinity-induced noise (Beilby and Al Khazaaly 2009; Al Khazaaly and Beilby 2012).

ROS Concentration Measurements

The ROS measurements confirmed that the melatonin pretreatment substantially decreased the ROS concentration in both sorbitol and saline APW (Fig. 6a). Melatonin antioxidant activity occurs via ROS scavenging cascade through AFMK (N_1-acetyl-N_2-formyl-5-methoxykynuramine) and AMK (N-acetyl-5-methoxykynuramine - kynuric pathway of melatonin metabolism) or indirectly by enhancing the activity of other free radical scavenging antioxidants or associated enzymes (Posmyk and Janas 2009; Tan et al. 2007b; Brown et al. 2012; Wang et al. 2012; Zhang et al. 2013). However, the ROS concentration was not higher in saline APW and the timing measurement (Fig. 6b) confirmed that ROS production in the cell actually dropped following the exposure to saline APW. Li et al. (2007) measured H_2O_2 concentration in rice roots exposed to saline. They found an oxidative burst in the first 15 min of saline stress, followed by a decline to $\sim$50 % of control, as the antioxidant activity increased. However, in prolonged stress (more than an hour), the ROS concentration started to increase again as the antioxidant production failed. Thus, the H^+/OH^- channel noise in *Chara* might be activated by the initial oxidative burst (which is not resolved by our measurements). The global H^+/OH^- channel opening might later follow as ROS concentration starts to increase again. Alternatively, ROS also acts as signaling molecule (Miller et al. 2010) and some downstream substance activated by ROS might open the H^+/OH^- channels. Presoaking cells in melatonin APW for 24 h increased endogenous melatonin concentration (Lazar et al. 2013) and prevented or diminished the oxidative burst and subsequent ROS signaling upon exposure to saline APW. Thus, the H^+/OH^- channels were not activated or activated with a time delay and their co-operativity was affected leading to isolated spikes in the membrane PD data (Fig. 5). Future research is planned to resolve the rate of production of ROS as a function of time in saline medium.

Are H^+/OH^- channels relevant to plants in general? The complex electrophysiological motif of H^+/OH^- channels and their spatial juxtaposition with the proton pump were found in aquatic angiosperms (Prins et al. 1980), pollen tubes (Feijo et al. 1999) and roots of land plants (Raven 1991). In the roots the protons are pumped out in the acid root subapical zone, while the H^+/OH^- channels are open at the alkaline root tip (Raven 1991). Raven suggests that this pH banding facilitates acquisition of molybdenum, phosphorus and iron as well as reduction of aluminium toxicity. Tyerman et al (2001) measured current-voltage characteristics in protoplasts from wheat roots and these could be modeled by pump-dominated or H^+/OH^- channel dominated membrane states. Further, Tyerman et al (1997) observed salinity-induced noise in wheat root protoplasts. Thus H^+/OH^- channels may be another parameter in salt tolerance/sensitivity and future experiments should investigate the effect of salinity on the acid/alkaline zones of roots of both glycophytes and halophytes.

Acknowledgments We thank P. Ranganathan and G. Craigie for assistance with the ROS experiments.

Conflict of interest Authors declare that they have no conflict of interest.

References

Al Khazaaly S (2011) Modelling electrophysiological responses of Characeae to salt and osmotic stress. Ph. D. thesis, School of Physics, The University of NSW, Sydney, Australia

Al Khazaaly S, Beilby MJ (2012) Zinc ion blocks H^+/OH^- channels in *Chara australis*. Plant Cell Environ 35:1380–1392

Al Khazaaly S, Walker NA, Beilby MJ, Shepherd VA (2009) Membrane potential fluctuations in *Chara australis*: a characteristic signature of high external sodium. Eur Biophys J 39:167–174

Amirjani MR (2010) Effect of NaCl on some physiological parameters of rice. Eur J Biol Sci 3:6–16

Beilby MJ, Al Khazaaly S (2009) The role of H^+/OH^- channels in salt stress response of *Chara australis*. J Membr Biol 230:21–34

Beilby MJ, Bisson MA (2012) pH banding in charophyte algae. In: Volkov A (ed) Plant electrophysiology: methods and cell electrophysiology. Springer Verlag, Heidelberg, pp 247–271

Beilby MJ, Casanova MT (2013) The physiology of Characean cells. Springer, New York

Bisson MA (1984) Calcium effects on electrogenic pump and passive permeability of the plasma membrane of *C. corallina*. J Membr Biol 81:59–67

Bisson MA, Walker NA (1980) The *Chara* plasmalemma at high pH. electrical measurements show rapid specific passive uniport of H^+ or OH^-. J Membr Biol 56:1–7

Bisson MA, Walker NA (1981) The hyperpolarisation of the *Chara* membrane at high pH: effects of external potassium, internal pH, and DCCD. J Exp Bot 32:951–971

Boccalandro HE, Gonzalez CV, Wunderlin DA, Silva MF (2011) Melatonin levels, determined by LC-ESI-MS/MS, fluctuate during the day/night cycle in *Vitis vinifera* cv Malbec: evidence of its antioxidant role in fruits. J Pineal Res 51:226–232

Brown PN, Turi CE, Shipley PR, Murch SJ (2012) Phytochemical discovery in large cranberry (*Vaccinium macrocarpon* Ait.) and small cranberry (*Vaccinium oxycoccus* L. and *Vaccinium vitis-idaea* L.) in British Columbia. Planta Med 78:1–11

Brzezinski A (1997) Melatonin in humans. N Engl J Med 336:186–195

Dubbels R, Reiter RJ, Klenke E, Goebel A, Schnakenberg E, Ehlers C, Schiwara HW, Schloot W (1995) Melatonin in edible plants

identified by radioimmunoassay and high-performance liquid chromatograph-mass spectrometry. J Pineal Res 18:28–31

Eremin A, Bulychev A, Hauser MJB (2013) Cyclosis-mediated transfer of H_2O_2 elicited by localized illumination of *Chara* cells and its relevance to the formation of pH bands. Protoplasma 250:1339–1349

Feijo J, Sainhas J, Hackett GR, Kunkel JG, Hepler PK (1999) Growing pollen tubes possess a constitutive alkaline band in the clear zone and a growth-dependent acidic tip. J Cell Biol 144:483–496

Hattori A, Migitaka H, Masayake I, Itoh M, Yamamoto K, Ohtani-Kaneko R, Hara M, Suzuki T, Reiter RJ (1995) Identification of melatonin in plant seed, its effects on plasma melatonin levels and binding to melatonin receptors in vertebrates. Int J Biochem Mol Biol 35:627–634

Hope AB, Walker NA (1975) The physiology of giant algal cells. Cambridge university press, London

Lazar D, Murch SJ, Beilby MJ, Al Khazaaly S (2013) Exogenous melatonin affects photosynthesis in Characeae *Chara australis*. Plant Signal Behav 8(3):23279

Li J-Y, Jiang A-L, Zhang W (2007) Salt stress-induced programmed cell death in rice root tip cells. J Integr Plant Biol 49:481–486

McCourt RM, Delwiche CF, Karol KG (2004) Charophyte algae and land plant origins. Trends Ecol Evol 19:661–666

Miller G, Suzuki N, Ciftci-Yilmaz S, Mittler R (2010) Reactive oxygen species homeostasis and signalling during drought and salinity stresses. Plant Cell Environ 33:453–467

Murch SJ, Saxena PK (2002) Melatonin: a potential regulator of plant growth and development. Dev Biol 38:531–536

Murch SJ, Simmons CB, Saxena PK (1997) Melatonin in feverfew and other medicinal plants. Lancet 350:1598–1599

Murch SJ, Krishnara JS, Saxena PK (2000) Tryptophan is a precursor for melatonin and serotonin biosynthesis in vitro regenerated St. John's wort (*Hypericum perforatum* L. cv. Anthos) plants. Plant Cell Rep 19:698–704

Murch SJ, Campbell SSB, Saxena PK (2001) The role of serotonin and melatonin in plant morphogenesis: regulation of auxin-induced root organogenesis in in vitro cultured explants of St. John's wort (*Hypericum perforatum* L.). In Vitro Cell Dev Biol 37:786–793

Murch SJ, Ali AR, Cao J, Saxena PK (2009) Melatonin and serotonin in flowers and fruits of *Datura metel* L. J Pineal Res 47:277–283

Murch SJ, Hall BA, Le CH, Saxena PK (2010) Changes in the levels of indoleamine phytochemicals in véraison and ripening of wine grapes. J Pineal Res 49:95–100

Pelagio-Flores R, Munoz-Parra E, Ortiz-Castro R, Lopez-Bucio J (2012) Melatonin regulates *Arabidopsis* root system architecture likely acting independently of auxin signaling. J Pineal Res 53:279–288

Poggeler B, Balzer I, Hardeland R, Lerchl A (2001) Pineal hormone melatonin oscillates also in the dinoflagellate *Gonyaulax polyedra*. Naturwissenschaften 78:268–269

Posmyk M, Janas K (2009) Melatonin in plants. Acta Physiol Plant 31:1–11

Prins HBA, Snel JFH, Helder RJ, Zanstra PE (1980) Photosynthetic HCO_3^- utilization and OH^- excretion in aquatic angiosperms. Plant Physiol 66:818–822

Raven JA (1991) Terrestrial rhizophytes and H^+ currents circulating over at least a millimeter: an obligate relationship? New Phytol 117:177–185

Shepherd VA, Beilby MJ, Al Khazaaly S, Shimmen T (2008) Mechano-perception in *Chara* cells: the influence of salinity and calcium on touch-activated receptor potentials, action potentials and ion transport. Plant Cell Environ 31:1575–1591

Shimmen T (2007) The sliding theory of cytoplasmic streaming: fifty years of progress. J Plant Res 120:31–43

Tan D-X, Manchester LC, Di Mascio P, Martinez GR, Prado FM, Reiter RJ (2007a) Novel rhythms of N^1-acetyl-N^2-formyl-5-methoxykynuramine and its precursor melatonin in water hyacinth: importance for phytoremediation. FASEB J 21:1724–1729

Tan D-X, Manchester LC, Terron MP, Flores LJ, Reiter RJ (2007b) One molecule, many derivatives: a never-ending interaction of melatonin with reactive oxygen and nitrogen species? J Pineal Res 42:28–42

Tan D-X, Hardeland R, Manchester LC, Korkmaz A, Ma S, Rosales-Corral SA, Reichle RA (2012) Functional roles of melatonin in plants, and perspectives in nutritional and agricultural science. J Exp Bot 63:577–597

Tan D-X, Manchester LC, Rosales-Corral SA, Acuna-Castroviejo D, Reiter RJ (2013) Mitochondria and chloroplasts as the original sites of melatonin synthesis: a hypothesis related to melatonin's primary function and evolution in eukaryotes. J Pineal Res 54:127–138

Timme RE, Bachvaroff TR, Delwiche ChF (2012) Broad phylogenomic sampling and the sister lineage of land plants. PloS ONE 7:29696

Tyerman S, Beilby MJ, Whittington J, Juswono U, Newman I, Shabala S (2001) Oscillations in proton transport revealed from simultaneous measurements of net current and net proton fluxes from isolated root protoplasts: MIFE meets patch-clamp. Aust J Plant Physiol 28:591–604

Tyerman S, Skerrett M, Garrill A, Findlay GP, Leigh RA (1997) Pathways for the permeation of Na^+, and Cl^- into protoplasts derived from the cortex of wheat roots. J Exp Bot 48:459–480

Van Tassel DL, Roberts N, Lewy A, O'Neil SD (2001) Melatonin in plant organs. J Pineal Res 31:8–15

Wang P, Yin L, Liang D, Li Ch, Ma F, Yue Z (2012) Delayed senescence of apple leaves by exogenous melatonin treatment: toward regulating the ascorbate–glutathione. J Pineal Res 53:11–20

Wodniok S, Brinkmann H, Glockner G, Heidel AJ, Philippe H, Melkonian M, Becker B (2011) Origin of land plants: do conjugating green algae hold the key? BMC Evol Biol 11:104–114

Wolf K, Kolar J, Witters E, van Dongen W, van Onckelen H, Machackova I (2001) Daily profile of melatonin levels in *Chenopodium rubrum* L. depends on photoperiod. J Plant Physiol 158:1491–1493

Wu L -J (2014) Voltage-gated proton channel H_V1 in microglia. The Neuroscientist online first http://nro.sagepub.com/content/early/2014/01/23/1073858413519864

Zhang N, Zhao B, Zhang H-J, Weeda S, Yang C, Yang Z-C, Ren S, Guo Y-D (2013) Melatonin promotes water-stress tolerance, lateral root formation, and seed germination in cucumber (*Cucumis sativus* L.). J Pineal Res 54:15–23